

# Explorative study on adaptive facades with superelastic antagonistic actuation

Filipe Amarante dos Santos<sup>1</sup>   Chiara Bedon<sup>2</sup>   Andrea Micheletti<sup>3</sup>

January 20, 2020

This is the pre-print of the paper “Explorative study on adaptive facades with superelastic antagonistic actuation” published in 10/01/2020, in Structural Control and Health Monitoring, with the DOI:

<https://doi.org/10.1002/stc.2463>.

<sup>1</sup> CERIS and Departamento de Engenharia Civil, Faculdade de Ciências e Tecnologia

Universidade NOVA de Lisboa

Quinta da Torre, 2829-516 Caparica, Portugal

*fpas@fct.unl.pt*

<sup>2</sup> Department of Engineering and Architecture

University of Trieste

Piazzale Europa 1, 34127 Trieste, Italy

*chiara.bedon@dia.units.it*

<sup>3</sup> Dipartimento di Ingegneria Civile e Ingegneria Informatica

University of Rome Tor Vergata

Via Politecnico 1, 00133, Rome, Italy

*micheletti@ing.uniroma2.it*

## Abstract

Glass facades and enclosures are highly attractive structures with increasing popularity between architects and engineers. These structures show very specific design requirements so as to guarantee an efficient interaction with the other building components. This is especially true in the case of “adaptive” glass systems, with continuously changing configurations according to a given design criteria. The main goal of this explorative study is the design of an adaptive facade module with antagonistic actuation. The geometry of the glazing system is controlled by pairs of superelastic

cables actuated against each other in a reversible way. Superelasticity is here exploited so as to improve the structural behavior of the facade system subjected to wind loads. The efficiency of the proposed design concept is demonstrated via Finite-Element numerical analyses and also from test data obtained from an experimental prototype. It is shown that the the proposed control approach can yield substantial structural enhancements and benefits for the adaptive facade module, which are substantiated by important reductions of maximum deformations and stresses in the cladding elements.

*Keywords: adaptive facades; glass panels; shape-memory alloys; superelastic behavior; antagonistic actuation.*

## 1 Introduction

The building industry is one of the largest consumers of material and energy resources, with a paramount impact on the environment. In order to minimize this impact there is a growing consensus that alternative strategies are needed optimize new construction and make it more sustainable. The basic design principles in which civil engineering structures rely are mostly based on the assumption that they need to comply with very stringent safety and serviceability criteria, associated with extremely demanding loadings but with a very low probability of occurrence. This means that, during most of their service lives, structures are effectively over designed [1, 2].

Structural adaptation fosters a new design paradigm in which strength and stiffness are controlled in real-time through sensing and actuation, to counteract loading effects [3]. By changing shape it is possible to achieve stress homogenization throughout the structure and to efficiently control its deformations. This way, structural design ceases to be controlled by rarely occurring loading events, resulting in significant material savings, reduction of environmental impact through energy minimization, and improved structural performance [2].

The topics of structural control and structural adaptiveness in facade engineering are becoming increasingly important. For instance, an innovative facade passive control approach making use of glass panels as passive absorbers, to reduce the effects of wind-induced vibrations on tall buildings,

was proposed in [4]. Also a democratization of more sophisticated control systems is taking place, due to the development of new robust open-source microcontrollers and a multitude of sensors based in Micro-Electro-Mechanical Systems, or MEMS. Adaptiveness in building envelopes is usually achieved by providing its facade elements with kinetic features, normally associated with movement and deformation.

With these kinetic features it is possible to improve the structural performance of a facade with respect to wind loadings by increasing the stiffness of the glass cladding elements through curvature modulation. The high flexibility of thin glass panels can be used advantageously for the implementation of such adaptive features. In fact, even though their inherent flexibility is responsible for their high deflections it also fosters the possibility to control their shape with limited force inputs. Thin glasses are conventionally recognized as glass layers having a maximum thickness of 2 mm. Thin glasses show flawless surfaces with very high quality, due the fact that they do not interact with any solid during the overflow-fusion process associated with their production. These glass layers are usually pre-stressed by chemical strengthening, increasing their surface compression up to a minimum of 230 MPa. According to specification sheets provided by some thin glass manufacturers, for example, Gorilla glass (Corning), Leoflex (AGC - Asahi Glass corporation) and Xensation (SCHOTT), chemical strengthened thin glass elements achieve compressive strengths as high as 900 MPa [5, 6].

In Figure 1 are depicted some of the kinetic features explored in adaptive facades, associated with the movement (translation/rotation) and deformation of the panel. As in adaptive systems in nature, that continuously adapt to external stimuli including variations in light, temperature, humidity or pressure, these features can also be used to create controllable openings, to improve the energy efficiency of the building.

The simplest expression of a curved shell shape is the single-curvature shell with a circular based cross section, shown in Figure 1(a). A primary factor in the structural design of a shell structure is the degree to which the system carries loads through in-plane membrane stresses as opposed to combinations of bending and shearing stresses. A short single-curvature shell shows a hybrid behavior between a vault and plate.

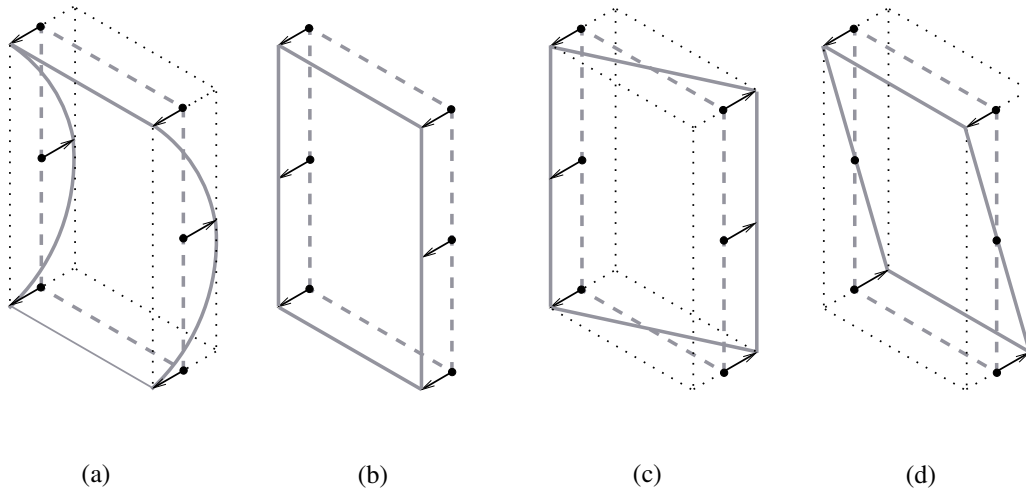


Figure 1: Kinetic features associated with adaptive actuation in glass panels. Legend: a - introduction of single curvature; b - translation; c - rotation along vertical axis; d - rotation along horizontal axis.

In the design process, the movement geometry of structural elements is aimed, as a general rule, at leading to the lowest degree of complexity to obtain simple and, therefore, robust and durable constructions. Shape-memory alloy cable elements substantiate one of simplest forms of mechanical actuators since the driving force is provided by the material itself, with no complicated moving parts.

Most of the actuated structures using SMA elements are based in thermally driven one-way shape-memory based actuators, which have to rely on bias force-creating components in order to restore their initial shape, since they do not recover their original configuration upon cooling. One of the methods to provide the bias force, obtaining reversible-actuation systems, is to use an antagonistic type of actuation, inspired by muscles that work in pairs [7, 8, 9, 10, 11, 12, 13]. An antagonistic actuation requires the assembly of two opposing SMA active elements in which the contraction (upon heating) of one pre-stressed actuator causes the opposing actuator to stretch, arming it to a subsequent heating. One of the main advantages of these antagonistic devices is the fact that they not need continuous power, but just an electric pulse, to switch permanently to a new configuration. In the present work, the actuating principle is based on the superelastic effect (reversible strain change upon loading-unloading at temperatures above the Austenite finish temperature  $A_f$ ). Reversible morphing structures utilizing pre-strained superelastic

SMA cables as linear actuating elements take advantage not only of the stress plateau but also of the stress hysteresis and temperature dependence of superelasticity, by exploiting the reversible transformation between austenite and stress-induced martensite brought about by a heating-cooling pulse. We refer the reader to [7] for an introduction on antagonistic superelastic actuation.

The actuation principle of a two-element antagonistic system is associated with the ‘butterfly diagram’ represented in Figure 2 (bottom). When the element SMA1 is subjected to an heating-cooling pulse (top), the tensile stress in both elements increases and then decreases, while the displacement changes upon heating ( $A \rightarrow B$ ) and cooling ( $B \rightarrow C$ ). When the the element SMA2 is subsequently subjected to an heating-cooling pulse (bottom), the tensile stress in both elements increases and then decreases, while the displacement changes upon heating ( $C \rightarrow D$ ) and cooling ( $D \rightarrow E$ ). The displacement of the actuated point varies among A-C-E upon thermal pulsing, without the need of heating any SMA element continuously.

## 2 Facade panel with antagonistic actuation

In order to adequately implement the described antagonistic actuation scheme in a facade panel, a point-fixed system is proposed, providing for optimum transparency with any given supporting structure. In the case of structural glass facades, specially designed bolts are usually inserted through perforations in the glass material and mate with a fitting that ties to the supporting structure. The implementation of the superelastic antagonistic actuator on a facade panel can be materialized by the functional scheme presented in Figure 3 (a), with the cables on both sides of the panel. An alternative functional scheme for the antagonistic actuation of a facade panel is presented in Figure 3 (b) that enables to have the cables all on the same side of the panel. For the present work, a six-point fixing system is used, comprising six antagonistic pairs of pre-strained superelastic cable elements, like the one shown in Figure 3 (c).

With the proposed six-degrees-of-freedom system it is possible to develop an adaptive facade element with all the kinetic features described in Figure 1. By defining appropriate activation setups, for the different antagonistic pairs, one can easily convey the facade panel with a single curvature, a translational movement or a rotation.

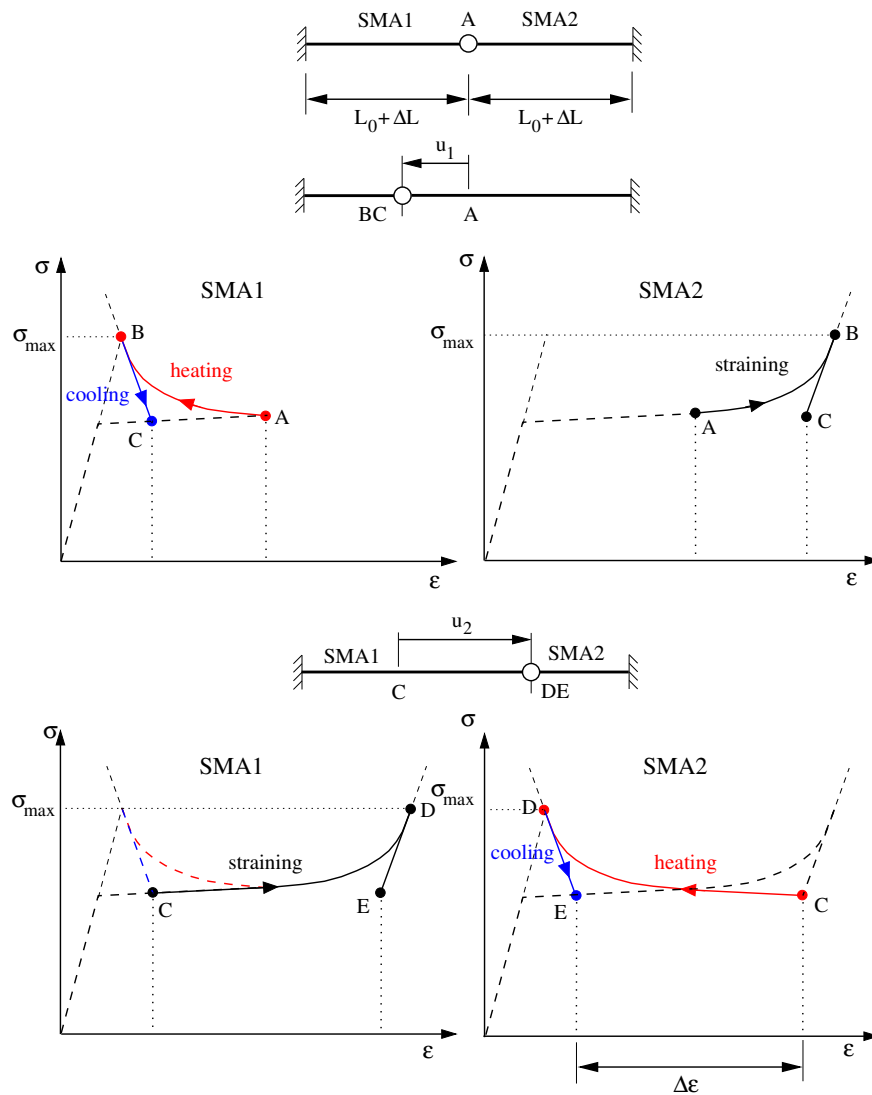


Figure 2: Actuation of antagonistic device with pre-strained elements SMA1 and SMA2 by heating-cooling pulses.

In Figure 4 are depicted the power activation sequences required to enforce these configurations in a facade element and to bring it back to its original state. Although it is possible to pulse the actuators to reach any target displacement using a feedback control system, the simplest version of our actuation method consists in having just two positions for each antagonistic pair, which suffices to obtain all schemes in Figure 4, and in such case feedback control is not necessary. Since a calibrated heating pulse applied to one SMA cable can consistently bring the other SMA cable on the martensitic branch of the sigma-epsilon plot (points B and D in Figure 2), the system yield

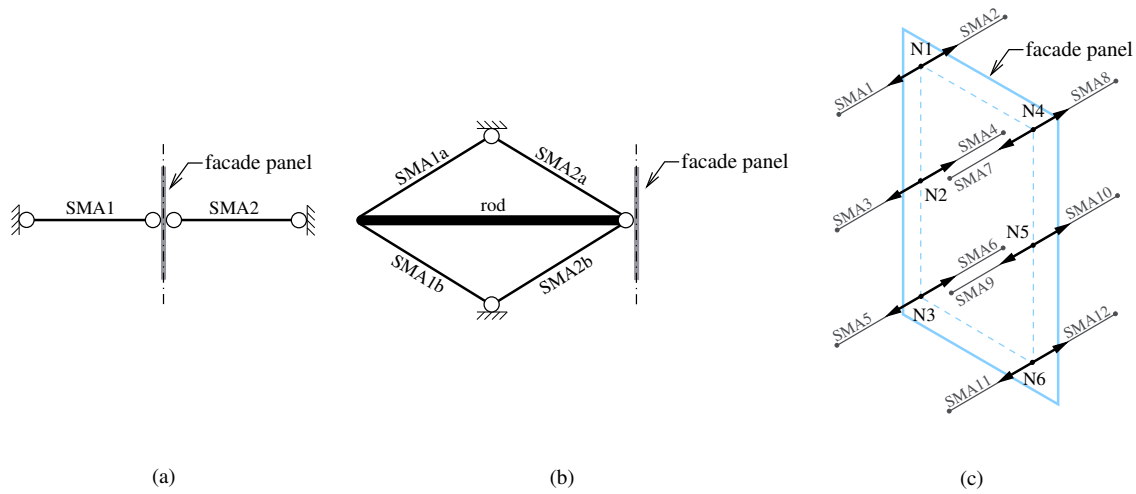


Figure 3: General layout of the adaptive facade system. (a) System with the cables on both sides of the facade element (b) System with the cables all on one side (c) A single glass panel equipped with SMA cables.

precisely the same exact displacement (corresponding to points C and E in Figure 2), after the pulsed cable cools down. In Figure 4 are shown which SMA cables need to be activated in order to obtain the different kinetic features for the facade panels. When actuated, since the same heat pulse is consistently used, the cables yield precisely the same exact displacement. One draws attention to the fact that power input is only required to change the configuration of the system (steps (a) and (c) of Figure 4). When the system is switched off (steps (b) and (d) of Figure 4) the facade element is able to maintain the desired shape. This is one of the main advantages of the proposed actuation principle: it does not need a continuous power input to keep a given configuration.

A small scale experimental prototype was built to test the feasibility the proposed adaptive facade actuation principle, based in sets of antagonistic SMA cables. A  $400 \times 250 \text{ mm}^2$  acrylic panel with a nominal thickness of 2.5 mm was used. The panel was suspended by six pairs of 200 mm long superelastic cables, with a diameter of 0.1 mm. Figures 5 and 6 show the layout and the general view of the experimental prototype, respectively.

The superelastic cables were clamped to the panel by a series of SMA cable clamps. At the opposite extremity, the superelastic cables were clamped to specially designed SMA cable strainers, that enabled the introduction of pre-strain in the cables. The SMA cables were heated through Joule effect by twelve 9 V batteries, placed at the vicinity of each cable. These batteries were inde-



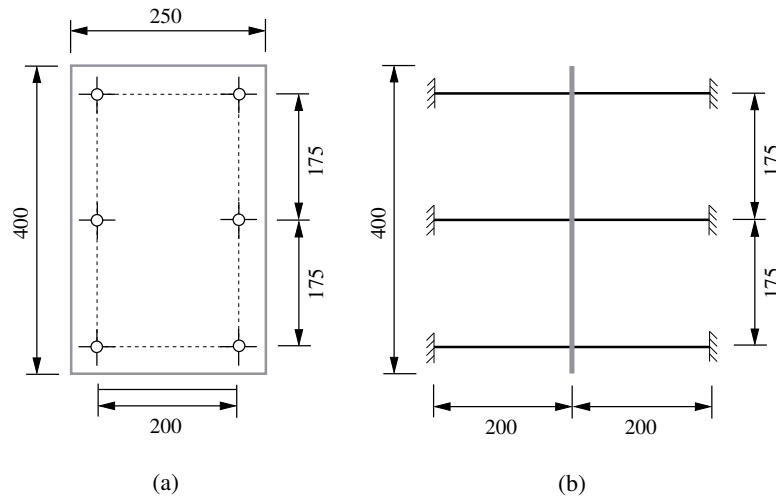


Figure 5: Nominal dimensions of the adaptive facade module. (a) Front view (b) Lateral view (all dimensions are given in mm).

diameters and Polyactic acid (PLA) 3D-printed connectors. Also the cable clamps and the cable strainers were 3D-printed with PLA filament, using a PRUSA i3-MK2 printer.

The voltage time-history for an antagonistic SMA pair is depicted in Figure 7, for a duty cycle of the experimental prototype. In Figure 8 is shown the experimental prototype during the introduction of the kinetic features presented in Figure 1. One can easily acknowledge the efficacy of the proposed superelastic antagonistic actuation scheme, which yielded a maximum displacement of 9 mm (measured through the length variation of the SMA cables).

As already mentioned, the proposed actuation system is based on the heating and cooling of a set of SMA wires. Heating is controlled by the introduction of an electrical current in the wires, which, through Joule effect, allows to heat the wires rather fast (for the tested experimental prototype it was possible to heat the wires within the period of a second). For cooling, the system relies on the free-convection heat-transfer mechanism between the surrounding fluid, which is air, and the SMA wires themselves. This free-convection heat-transfer mechanism mainly depends on the temperature difference between the wires and the surrounding air, on the diameter of the wires and on their relative position within the fluid. In the proposed application, the SMA wires are placed horizontally, which increases the efficiency of the heat-transfer mechanism and minimizes the duration of the time interval between two consecutive heatings. We exclude the possibility of

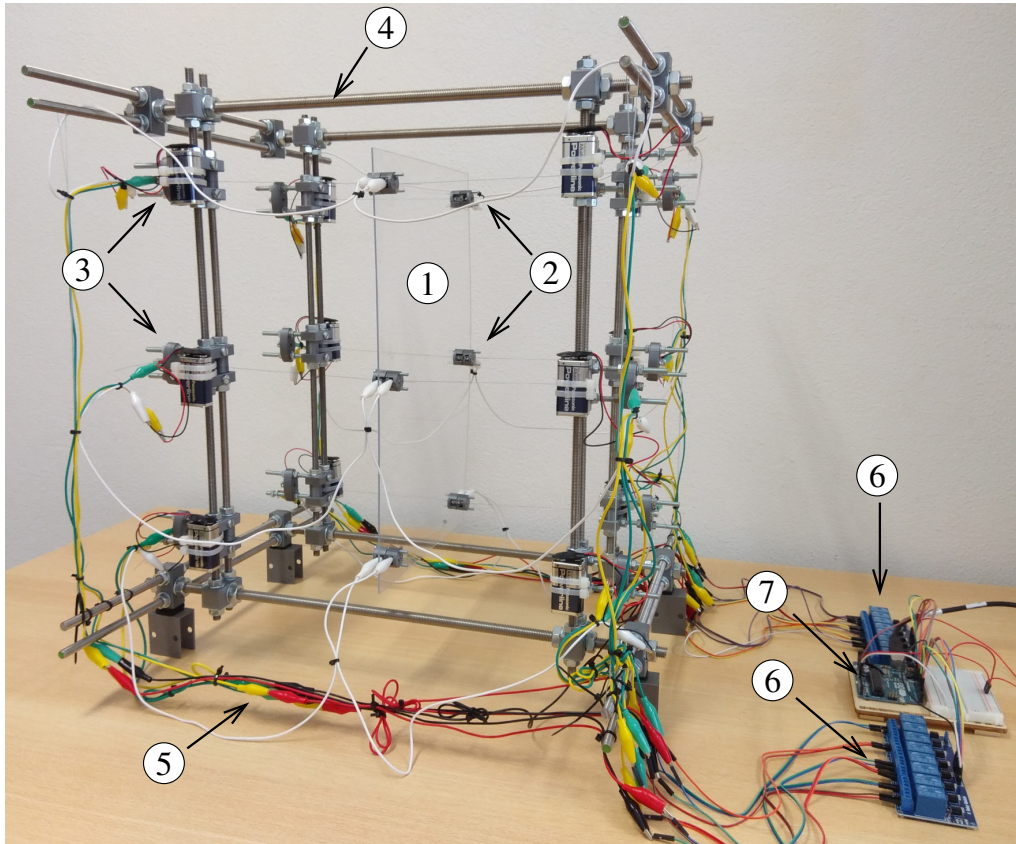


Figure 6: General view of the experimental prototype. Legend: 1 - acrylic panel; 2 - SMA cable clamps; 3 - SMA cable strainers with power supplies; 4 - main frame; 5 - electrical cable wiring; 6 - relay modules; 7 - arduino UNO.

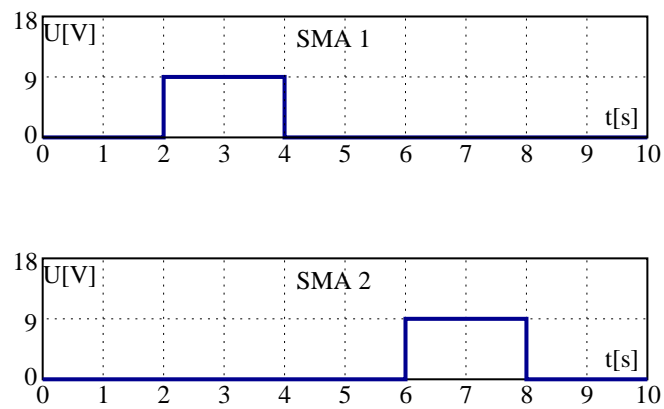


Figure 7: Voltage time-history in the SMA cables during a duty cycle.

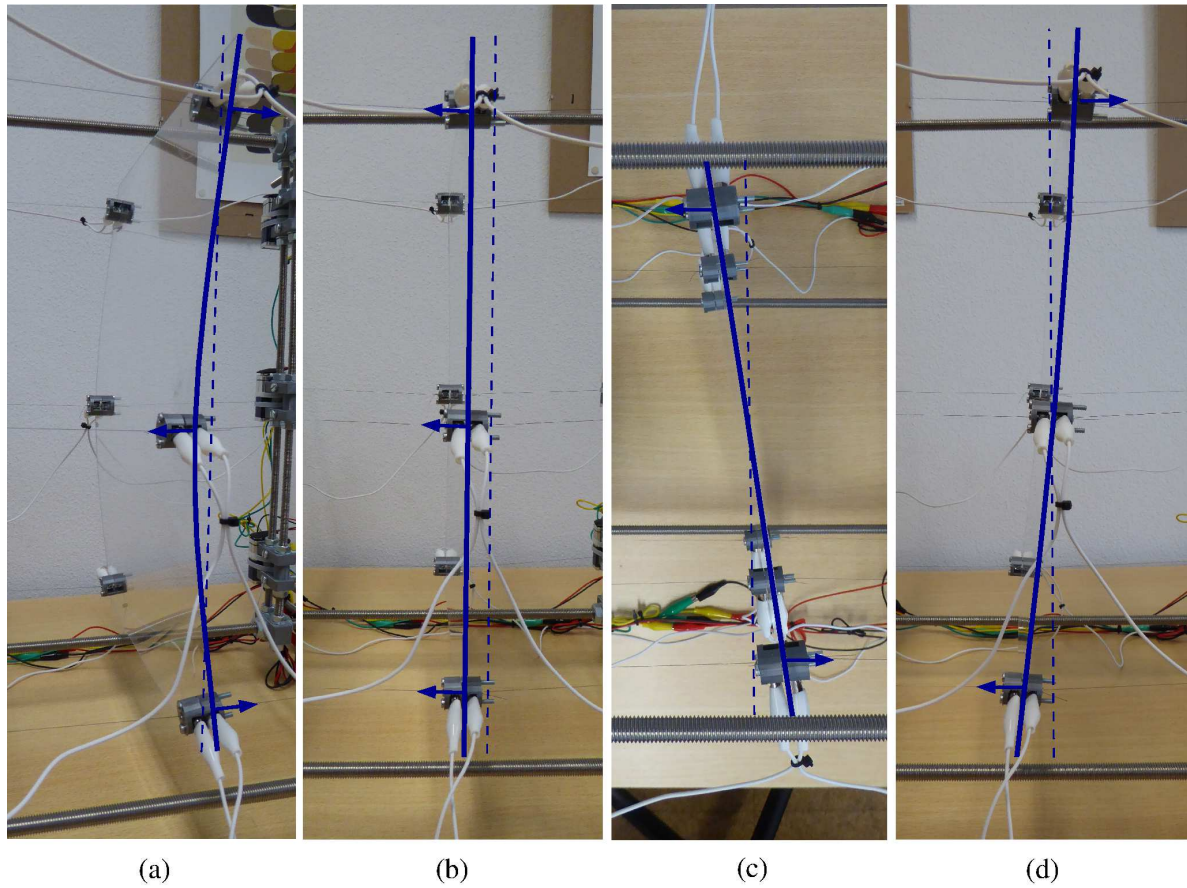


Figure 8: Experimental kinetic features associated with adaptive actuation in the small-scale acrylic panel. Legend: a - single curvature (lateral view); b - translation (lateral view); c - rotation along vertical axis (top view); d - rotation along horizontal axis (lateral view).

implementing a forced convection mechanism (for instance, with the use of mechanical fans) since this would add an unnecessary complication to the system.

One draws attention to the fact that the performance of the system is not really hindered by the physical limitations associated with the convective cooling process since the system is not designed to work in a fast dynamic regime. The idea is to change the configuration of the system when needed, in response to a particular energetic or structural efficiency demand. We are assuming that the user needs to move the structure back or to another configuration after a period of time larger than the cooling time. The large change of configuration due to wire heating happens rapidly (path CD in Figure 2). Then cooling takes place slowly (for the experimental prototype cooling took approximately 2 seconds), with a small change in configuration (path DE in Figure 2).

Due to the specific nature of the proposed actuation scheme, the operational life of the SMA adaptive components is mostly controlled by transformation (or functional) fatigue rather than by structural fatigue, which is associated with fracture due to stress or strain cycling at constant temperature[14]. Transformation fatigue occurs every time the SMA element works as an actuator, describing the gradual loss of its ability to generate mechanical stress under constrained conditions. Two of the most important parameters affecting the NiTi wire functional fatigue are the number of transformation cycles and the heating time during each cycle. By using heat pulses to activate the SMA wires it is possible to enhance their functional fatigue behavior by preventing overheating [15]. In addition, it has been shown in [16] that it is possible to obtain repeatable motion from SMA wires working as actuators for tens of millions of cycles by limiting the imposed strains up to 5%. When the strains and stresses are higher, a good cyclic behavior can only be obtained for hundreds or a few thousand cycles [16].

### 3 Curvature modulation for stiffness control

Numerical simulations were carried out to assess the effectiveness of the proposed adaptive approach regarding the curvature modulation of a facade panel to control its stiffness. SAP2000 was used to build up the finite-element (FE) models, comprising four-node quadrilateral shell elements with six degrees of freedom per node for the facade panels. The panels were simply supported at

the prescribed fixing points, and the displacements introduced by the SMA cables in the facade panel were simulated by imposing nodal displacements. Nonlinear static analyses were performed considering P-Delta effects (with large-displacements) and the geometric stiffness.

### 3.1 Small-scale acrylic panel

One of the goals of the present study was to stiffen the cladding element, when the facade is subjected to an ordinary wind pressure, by introducing a single curvature into the facade panel. To study the feasibility of this approach, a FE model of the small-scale experimental prototype was defined, with geometrical and mechanical properties equal to those of the prototype. A pre-camber (see Figure 9) was hence introduced in the of the acrylic panel (through nodal displacements simulating the SMA actuation system), up to a maximum value of 10 mm, as a pressure of 1.0 kN/m<sup>2</sup> was applied to simulate the wind design load in service conditions. Values of 3.0 GPa and 0.37 were considered for the Young's modulus and the Poisson coefficient of the acrylic panel. The self-weight of the panel was neglected in the FE analysis. This is due to the fact that, in facade engineering, it is usual to suspend the self-weight of the panels through dedicated vertical cables that would have to be added to the system.

In Figure 9 are depicted the displacements for the acrylic panel, as obtained from the FE numerical model. In Figure 9 (a) are shown the displacements of the flat panel when subjected to the prescribed wind pressure. As shown, the six point-supported panel deforms with a maximum deflection of about 3.75 mm. In Figure 9 (b) the out-of-plane displacements associated with the introduction of a 6 mm pre-camber are presented. In Figure 9 (c) are shown the total displacements shown by the curved panel when subjected to the pre-camber and subsequent wind loading. Finally, in Figure 9 (d), is presented the response of the curved panel in terms of deformation increments due to the wind pressure only.

By observing Figure 9, one can easily acknowledge that the introduction of a single curvature in the acrylic panel allows for a substantial increase in stiffened, with decrease of the maximum wind displacements from 3.75 mm to 1 mm, which represents a reduction of 73 %, with respect to the original out-of-plane displacement. However, such a global benefit/effect is strictly related to

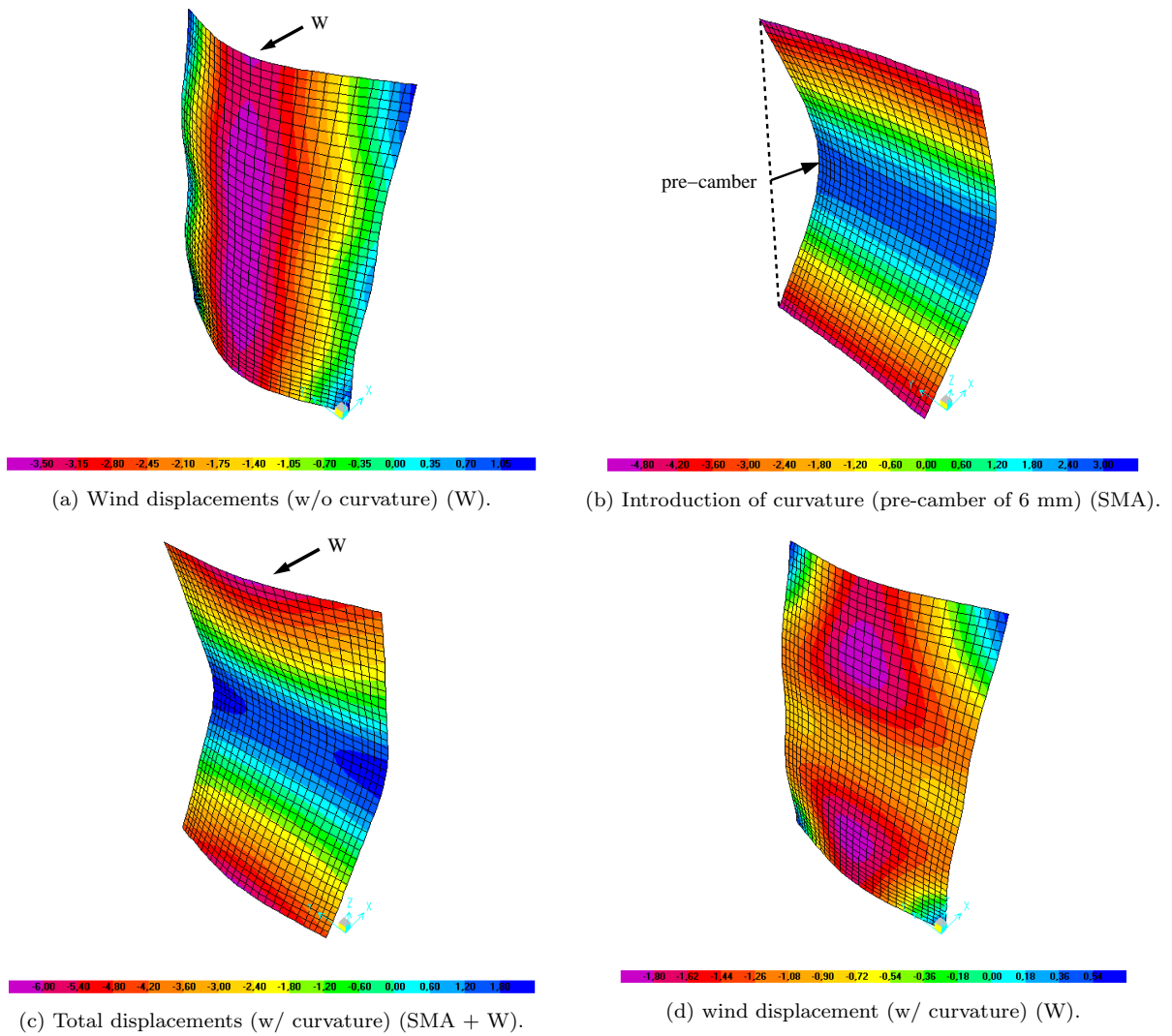


Figure 9: Displacements of the acrylic panel [mm].

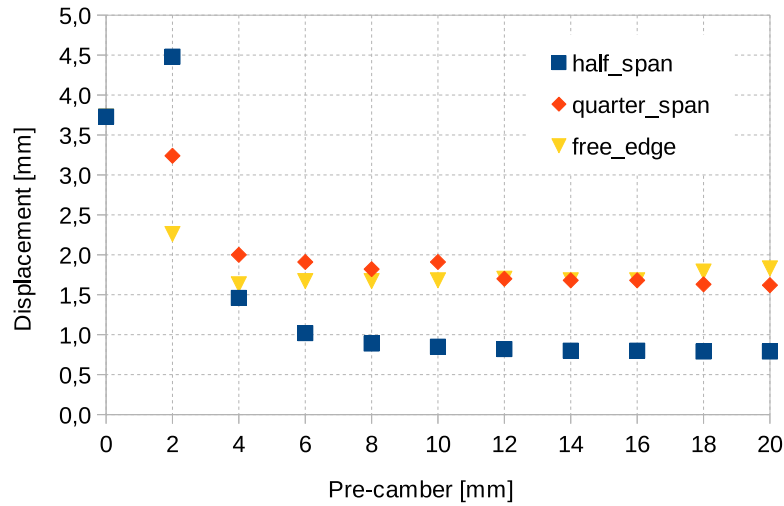


Figure 10: Displacement vs. pre-camber in the acrylic panel.

some input assumptions, i.e. the panel size, the number of point-supports and - for the examined panel - the imposed pre-camber amplitude. According to Figure 10, for example, it is possible to monitor the maximum out-of plane displacements of the acrylic panel, when subjected to the prescribed wind pressure, by changing the tested pre-camber amplitudes. The displacement results are proposed for three control points of the panel, namely corresponding to the half-span (centre of the panel), the quarter-span (centre of the panel) and the unrestrained top edge (mid-span section) of the panel.

One can see that the introduction of the pre-camber, and associated curvature, can markedly improve the behavior of the acrylic panel towards the service wind pressure, as the maximum displacement shown by the panel decreases down to 0.8 mm (for a pre-camber of 20.0 mm). At the same time, it is possible to notice that the maximum expected benefits tend to stabilize - for the examined system - as far as the pre-camber amplitude is equal or larger than 6.0 mm. Worth of interest, in the same figure, is the global response of the panel, as resulting from a combination of multiple geometrical and mechanical aspects. For pre-camber amplitudes larger than 12 mm, for example, the global deformed shape of the panel tends to change, with maximum out-of-plane deformations at the short edges of the sample.

### 3.2 Real-scale thin-glass panel

In order to validate the proposed approach for stiffness control through curvature modulation in a real scale facade module, a FE element model of a thin glass panel with  $2000 \times 1250 \text{ mm}^2$  and a thickness of 2.0 mm was studied. A six point suspension scheme was also adopted for the glass panel, similar to the one used with the acrylic panel. A wind design load of  $1.0 \text{ kN/m}^2$  was also used for this study. Values of 75.0 GPa and 0.22 were considered for the Young's modulus and the Poisson coefficient of the glass panel. The self-weight of the glass panel was also neglected, as in the previous study.

In Figure 11 is depicted the behavior of the thin glass panel subjected to the prescribed wind loading. One can see that, by introducing a pre-camber of only 6 mm, it is possible to eliminate the wind displacement of 230 mm at half-span, also decreasing its value to 50 mm at the quarter span and the free edge. In Figure 12 are shown the maximum and minimum stresses for the thin glass panel without curvature, when subjected to the prescribed wind loading. In Figure 13 are shown the maximum and minimum stresses for the thin glass panel associated with the introduction of a 6 mm pre-camber. One can see that due to the limited pre-camber, the stresses are very low. In Figure 14 one can assess the effect of the curvature in the stress distribution throughout the glass panel, by combining the pre-camber and the wind loading. One can see that, when the single curvature is introduced, a stress homogenization occurs throughout the thin glass panel, with the maximum and minimum stress levels decreasing from 315 MPa and -245 MPa to 210 MPa and -160 MPa, respectively. In order to clarify the influence of the curvature on the non-linear geometric behavior of the thin glass panel with the proposed dimensions, an additional set of pre-cambers was also tested, ranging up to 20 mm. In Figure 15 and Figure 16 are shown the results obtained with this parametric study, both in terms of displacements and stresses in the glass panel, respectively.

Finally, in order to apprehend the influence of the geometry of the panel, in terms of the relation between its length ( $l$ ) and width ( $w$ ), in the performance of the thin glass panel with a single curvature subjected to a wind loading, an additional parametric study was performed, considering variations on the geometry of the panel ranging from  $w/l = 0.250$  (rectangular panel with  $500 \times 2000 \text{ mm}^2$ ) up to  $w/l = 1$  (square panel with  $2000 \times 2000 \text{ mm}^2$ ). The results obtained

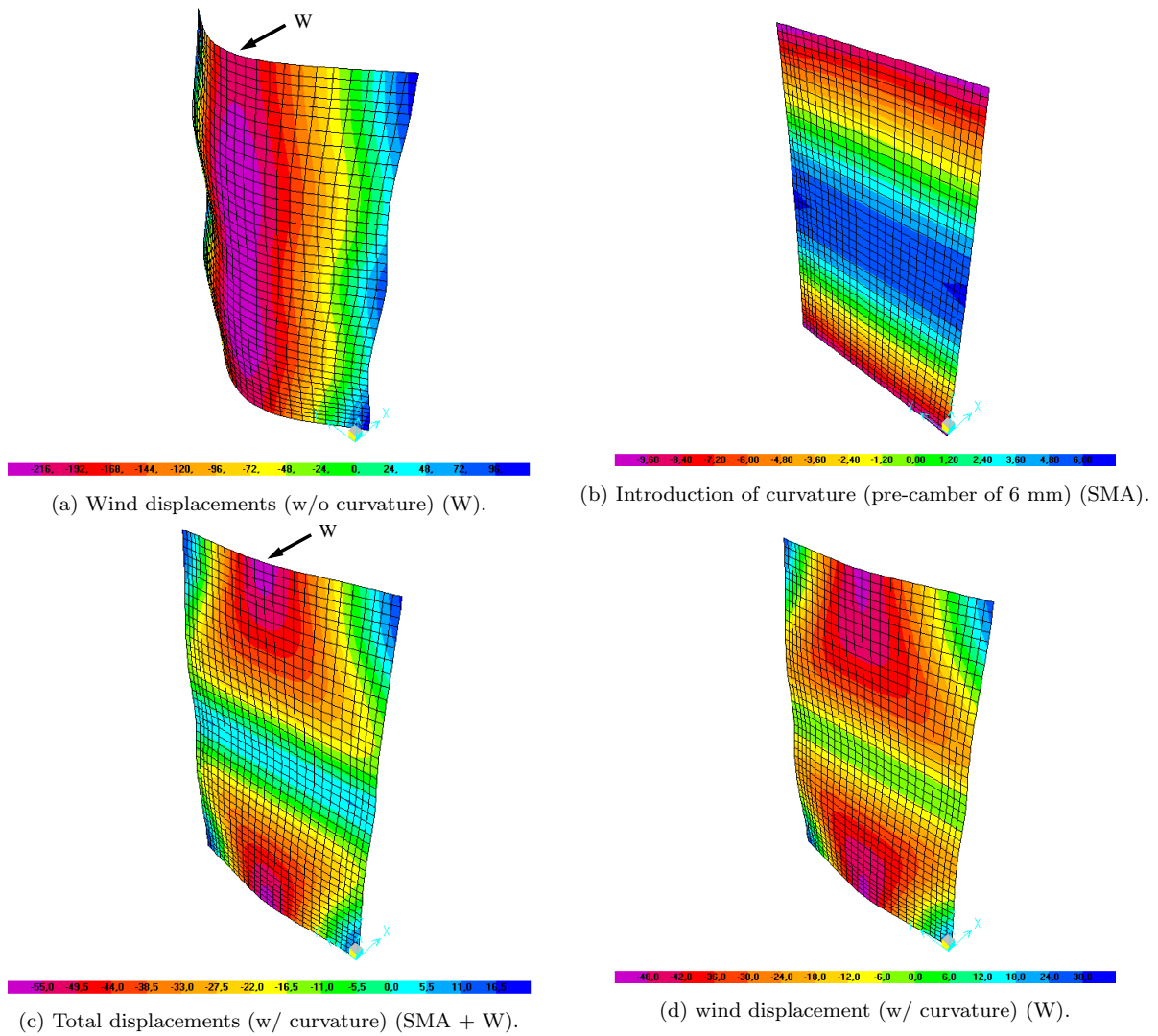


Figure 11: Displacements of the thin glass panel [mm]

in this parametric study are compiled in graphs presented in Figures 17 and 18, both in terms of displacements and stresses, respectively. In the horizontal axis are plotted the central displacement of the thin glass panel and the corresponding pre-camber.

One can see that both the wind displacements and stresses of the thin glass panel decrease as the initial pre-camber (curvature) increases, and that this reduction is more important as the  $w/l$  ratio increases. It is worth noticing that in the parametric studies related to the real-scale facade modules the value of the required pre-camber is extremely reduced, in comparison with the overall size of the panel. An optimized value of 6 mm was obtained for the pre-camber,

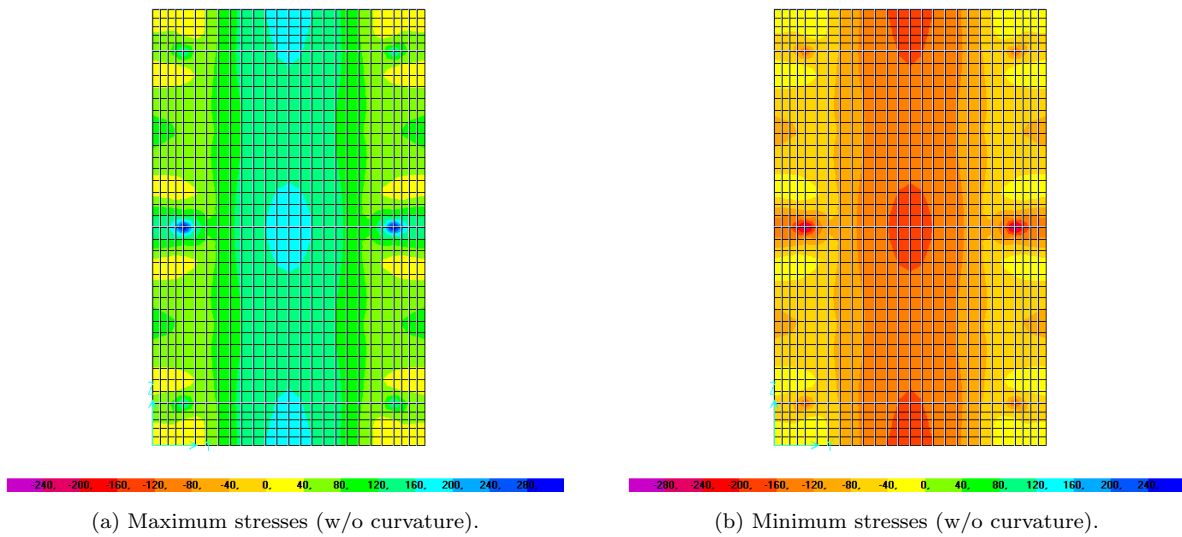


Figure 12: Wind stresses in the thin glass panel (W) [MPa].

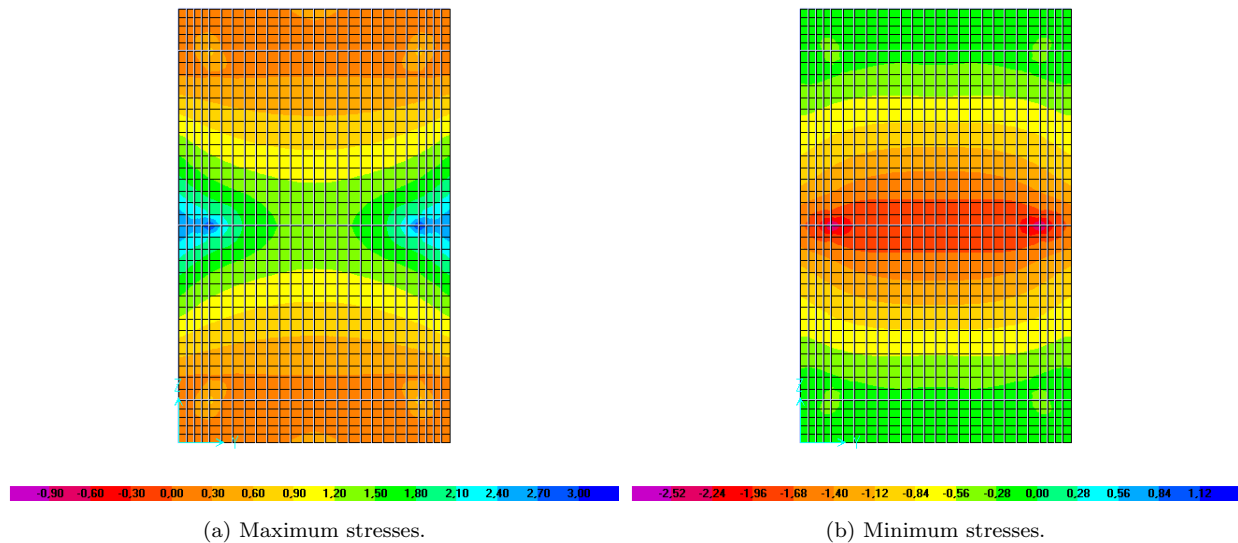


Figure 13: Pre-camber stresses in the thin glass panel (6 mm) (SMA) [MPa].

which represents only 1.2% of the shorter side of the considered panels (500 mm). We hence assumed that this limited amount of curvature does not yield significant changes in the aerodynamic wind pressure. More importantly, the higher stiffness of the panels associated with this curvature reduces wind dynamic effects. Figure 19 shows a depiction of a facade comprising several adaptive

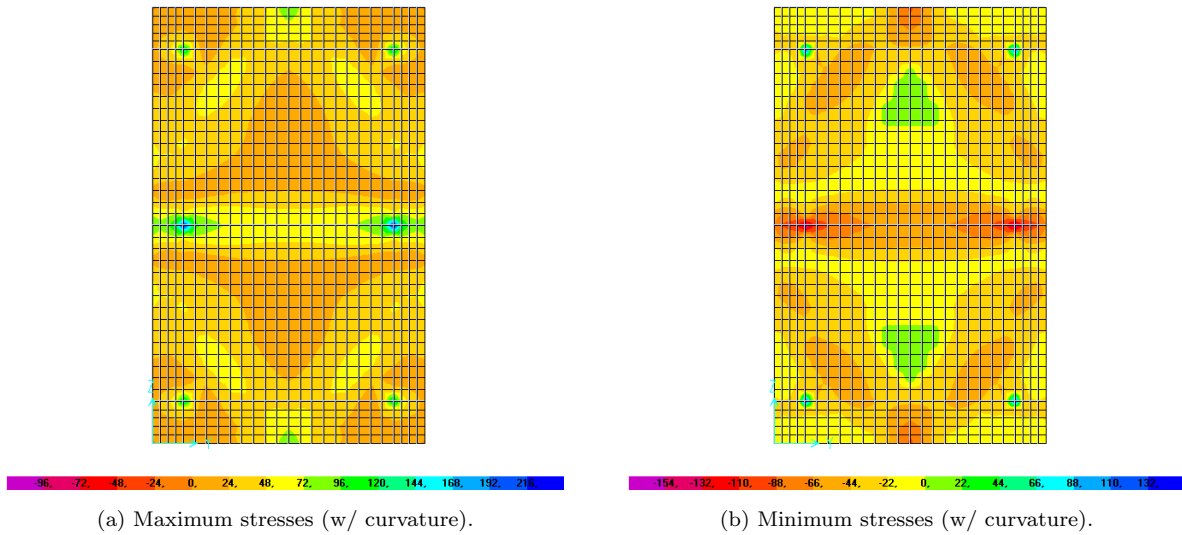


Figure 14: Total stresses shown by the thin glass panel (SMA + W) [MPa].

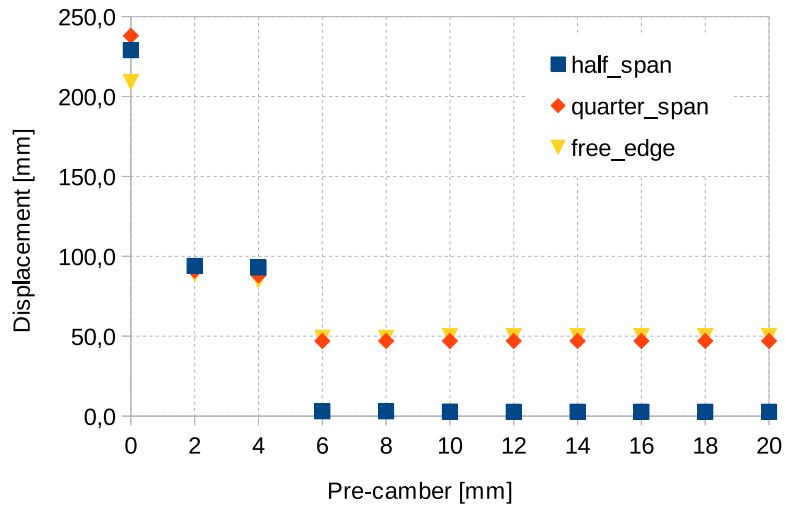


Figure 15: Displacement vs. pre-camber in the glass panel.

modules. As adjacent glass panels will be provided with the same amount of pre-camber, the relative displacement between panels will be negligible. Furthermore, as the expected pre-camber will be very limited the joints between panels or with the supporting frame can be easily designed to accommodate the corresponding edge displacements.

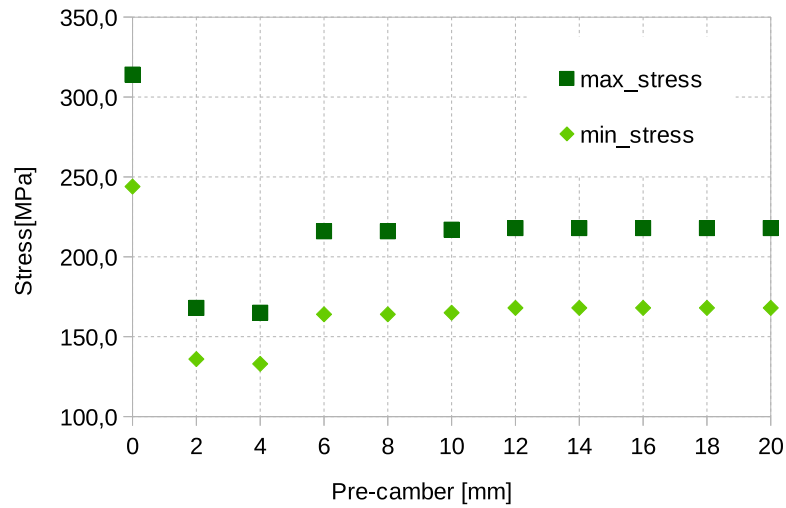


Figure 16: Stress vs. pre-camber in the glass panel.

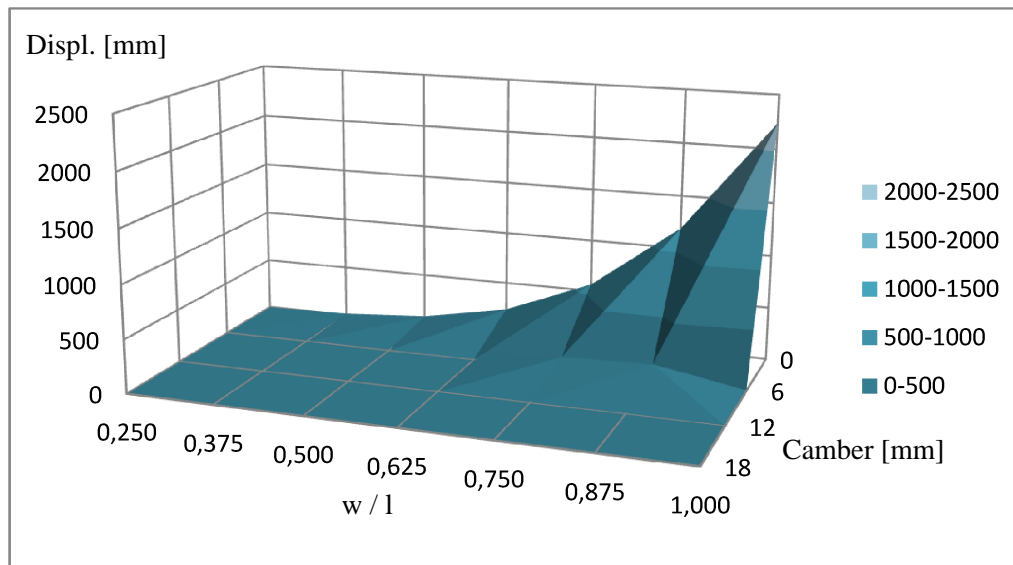


Figure 17: Central displacement [mm] vs. pre-camber [mm] vs.  $w/l$ .

## 4 Conclusions

In this paper, a novel design concept for an antagonistic actuation system was explored, via Finite-Element numerical simulations and a proof-of-concept prototype. Point-supported facade panels were considered in the study, where the transparency of cladding elements is maximized by means of limited mechanical restraints and frameless solutions. Thin glass panels were then taken into

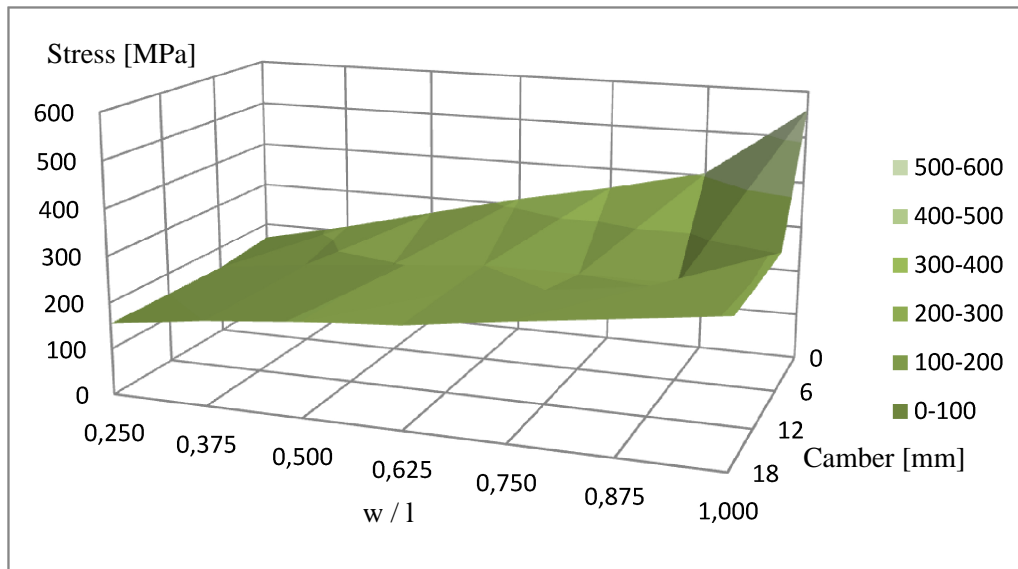


Figure 18: Maximum stress [MPa] vs. pre-camber [mm] vs.  $w/l$ .

account to assess feasibility and potential of a novel concept comprising SMA cables in facade modules adaptivity. The key aspects of the antagonistic actuation system relates to superelasticity as well as to the intrinsic flexibility of thin glass layers currently available on the market. As far as the input parameters of the antagonistic actuation system are set, the facade adaptivity can be emphasised in the form of switchable cladding components able to preserve their original transparency, and to ensure the additional advantages of shape/form changes. From a structural point of view, the same antagonistic actuation system can offer important benefits for the facade elements, being able to sustain limited deformations when subjected to ordinary design loads (i.e, wind pressure), as well as limited maximum stresses. One of the issues to be carefully considered, in order to deliver a fully operational adaptive facade module with superelastic antagonistic actuation, is the correct design of the SMA actuating cables: to obtain an adequate performance for this type of system, it is necessary to limit the stress variations in the SMA cables associated with wind loads, so that no martensitic stress-induced phase transformation occur in superelastic cables. The proposed actuation scheme for adaptive facades can be used without any thickness constraints whatsoever for kinetic applications associated with the translation and/or rotation of the facade panels (which can be made out of glass or of any alternative material), namely to create openings

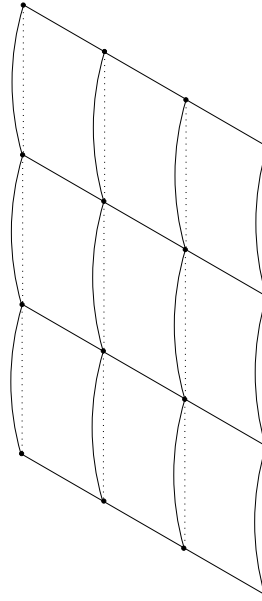


Figure 19: Depiction of a facade comprising several curved adaptive modules.

in the building envelope, to change its visual impact, or to realize adaptive sunshield systems, like in the case of Al Bahr Towers in the UAE [17]. It is only with the introduction of a curvature that the use of thin and flexible glass is mandatory. Although this innovative type of glasses are not yet popular in the construction industry, their use has already been proposed for facade applications [18, 19]. Following the numerical and experimental investigations summarised in the paper, and given the well-promising recorded behaviours, is it hence expected that the same design concept could be further explored in detail, so as to optimize it for full-scale applications. In the case of real applications, due to the presence of exogenous phenomena like temperature variations and wind pressure fluctuations, the implementation of a feedback control algorithm would be of paramount importance, in order to guarantee the accuracy of the control system. The study of such control scheme will be treated in future developments of the present work.

## Acknowledgements

We wish to thank the anonymous reviewers of a previous version of this article for providing helpful comments. AM gratefully acknowledges the financial support from the Italian Ministry of Education, University, and Research (MIUR) under the ‘FFABR’ grant L.232/2016.”

## References

- [1] P. O. Akadiri, E. A. Chinyio, and P. O. Olomolaiye, “Design of a sustainable building: A conceptual framework for implementing sustainability in the building sector,” *Buildings*, vol. 2, no. 2, pp. 126–152, 2012.
- [2] G. Senatore, P. Duffour, and P. Winslow, “Exploring the application domain of adaptive structures,” *Engineering Structures*, vol. 167, pp. 608 – 628, 2018.
- [3] F. Amarante dos Santos, A. Rodrigues, and A. Micheletti, “Design and experimental testing of an adaptive shape-morphing tensegrity structure, with frequency self-tuning capabilities, using shape-memory alloys,” *Smart Materials and Structures*, vol. 24, no. 10, p. 105008, 2015.
- [4] G. Pipitone, G. Barone, and A. Palmeri, “Optimal design of double-skin facades as vibration absorbers,” *Structural Control and Health Monitoring*, vol. 25, no. 2, p. e2086, 2018. e2086 stc.2086.
- [5] R. Silveira, C. Louter, and T. Klein, “Flexible transparency - a study on adaptive thin glass facade panels,” in *Challenging Glass Conference Proceedings*.
- [6] T. Weimar and A. Lopez, “Research on thin glass-polycarbonate composite panels,” in *Challenging Glass Conference Proceedings*, vol. 6, pp. 271–280, may 2018.
- [7] A. Micheletti, F. Amarante dos Santos, and P. Sittner, “Superelastic tensegrities: matrix formulation and antagonistic actuation,” *Smart Materials and Structures*, vol. 27, no. 10, p. 105028, 2018.
- [8] Z. Shi, T. Wang, and L. Da, “Performance analyses of antagonistic shape memory alloy actuators based on recovered strain,” *Smart Structures and Systems*, vol. 14, pp. 765–784, 2014.
- [9] T. Georges, V. Brailovski, and P. Terriault, “Characterization and design of antagonistic shape memory alloy actuators,” *Smart Materials and Structures*, vol. 21, p. 035010, 2012.

- [10] T. Ikeda, K. Sawamura, A. Senbab, and M. Tamayama, “Shape-retainment control using an antagonistic shape memory alloy system,” in *Active and Passive Smart Structures and Integrated Systems 2015, Proc. of SPIE Vol. 9431*, 2015.
- [11] C. Lai, C. Chu, and C. Lan, “A two-degrees-of-freedom miniature manipulator actuated by antagonistic shape memory alloys,” *Smart Materials and Structures*, vol. 22, p. 085006, 2013.
- [12] A. Sofla, D. Elzey, and H. Wadley, “Two-way antagonistic shape actuation based on the one-way shape memory effect,” *Journal of Intelligent Material Systems and Structures*, 2007.
- [13] T. Wang, Z. Shi, D. Liu, C. Ma, and Z. Zhang, “An accurately controlled antagonistic shape memory alloy actuator with self-sensing,” *Sensors*, vol. 12, pp. 7682–7700, 2012.
- [14] S. Casciati, L. Faravelli, and M. Vece, “Investigation on the fatigue performance of ni-ti thin wires,” *Structural Control and Health Monitoring*, vol. 24, no. 1, p. e1855, 2017.
- [15] P. Pappas, D. Bollas, J. Parthenios, V. Dracopoulos, and C. Galiotis, “Transformation fatigue and stress relaxation of shape memory alloy wires,” *Smart Materials and Structures*, vol. 16, pp. 2560–2570, 2007.
- [16] *Dynalloy: Technical characteristics of flexinol actuator wires.*
- [17] S. Attia, “Evaluation of adaptive facades: The case study of Al Bahr Towers in the UAE,” *QScience Connect*, vol. 2017, no. 2, 2018.
- [18] J. Neugebauer, M. Wallner-Novak, T. Lehner, C. Wrulich, and M. Baumgartner, “Movable Thin Glass Elements in Facades,” *Challenging Glass Conference Proceedings*, vol. 6, pp. 195–202, 2018.
- [19] P. Louter, M. Akilo, B. Miri, T. Neeskens, R. Ribeiro Silveira, O. Topcu, I. van der Weijde, C. Zha, M. Bilow, M. Turrin, T. Klein, and J. O’Callaghan, “Adaptive and composite thin glass concepts for architectural applications,” *Heron*, vol. 63, no. 1/2, 2018.